

Design and Performance Analysis of 28 GHz two-port MIMO Rectangular Microstrip Patch Antenna Array for 5G Applications

Shafiul Ismam¹, Delwar Hossain², and Syed Munimus Salam^{*2}
Muhammad Mahbubur Rashid³

^{1,2}*Dept. of EEE, Southern University, Chattagram, Bangladesh*

^{*2}*Dept. of EEE, USTC, Chattagram, Bangladesh*

³*Department of Mechatronics, Faculty of Engineering, International Islamic University Malaysia*

*Corresponding author: munim53@gmail.com

(Received: 9th September 2023; Accepted: 26th September 2023)

Abstract— A rectangular microstrip patch antenna array with two ports, designed for operation in the mm-wave band at 28 GHz for 5G applications, has been developed to exhibit superior gain and efficiency. This paper introduces a 12-element array activated by a feed network utilizing a T-junction power combiner/divider. The array elements consist of rectangular patch antennas inserted throughout the structure. The designed array antenna exhibited a measured impedance bandwidth of 1.42 GHz. The simulated findings indicate that the antenna achieved a favorable impedance match, with isolation levels below -22 dB throughout the frequency range. The whole substrate board dimensions were 19.99 × 26.968 × 0.254 mm³. The array is positioned on the substrate material known as Rogers RT5880, resulting in a consistent and reliable radiation pattern. The CST MWS software is employed to model and simulate the microstrip patch array antenna. CST MWS is an electromagnetic simulator utilizing the Finite Integration in Technique (FIT) methodology to model and analyze full-wave electromagnetic phenomena accurately. The realized gain of 15 dBi has been reached for the combined array, whereas the individual arrays have a realized gain of 12.3 dBi. The calculated overall efficiency is roughly -0.5 decibels. The antenna array under consideration has demonstrated favorable multiple-input multiple-output (MIMO) capabilities, as evidenced by an envelope correlation coefficient (ECC) of less than 0.1.

Keywords: *MIMO, 5G, and Antenna.*

1. INTRODUCTION

Antennas are fundamental components inside electric systems, establishing vital connections between transmitters and free space or between free space and receivers. Antennas play a crucial function in determining the properties of the system or device in which they are utilized. Antennas are utilized in various systems in diverse configurations. In specific systems, the operating parameters are intentionally aligned with the antennas' directional qualities or other relevant factors [1].

The ongoing progress in multimedia technology and the increasing demand for high-quality content and services have led to advancements in mobile communication, resulting in higher data capacity and faster speeds. As the rate at which data is transmitted and the number of mobile devices in use both experience exponential growth, the availability of frequency spectrum resources is becoming increasingly limited [2]. The forthcoming generation of cellular technology is poised to incorporate millimeter-wave (mm-Wave) bands, building upon the background. Due to the significantly wider bandwidth available in the mm-wave frequency spectrum compared to fourth generation/Long Term Evolution (4G/LTE) service, there is potential for substantial enhancements in data rate and capacity through a broader spectrum allocation.

The nascent technology necessitates antennas on user terminals that possess novel characteristics, including the ability to do spatial scanning through beamforming capabilities in their radiation patterns. This particular requirement presents a multitude of design challenges to strike a satisfactory balance between technological design considerations and commercial criteria. These criteria include cost-effectiveness, compact size, radiation efficiency, antenna gain, and broadband performance. Among the available options, microstrip antennas with coplanar arrangement of radiation elements and feeding network appear to be a favorable choice for achieving a functional component that offers a suitable combination of performance and manufacturing complexity, particularly for mobile applications [3].

The utilization of millimeter-wave (mmWave) carrier frequencies in forthcoming cellular networks and the implementation of high-gain adaptive antennas has been driven by the increasing need for high-speed cellular communications and the requirement for additional spectrum. The utilization of millimeter-wave channels has garnered significant interest due to their substantial bandwidth allocation. The user did not provide any text to rewrite.

The requirements of forthcoming mobile access technologies can be met by utilizing 5G mobile platforms. The U.S. Federal Communication Commission has undertaken an initiative to approve the utilization of licensed bands at frequencies of 28, 37, and 39 GHz as potential options for implementing 5G networks [5]. Designing antennas for frequencies of this magnitude presents various obstacles, yet it also has the advantage of occupying less physical area. As evidenced by empirical observations, the predominant design choice for 5G antennas is array structures. These designs effectively address the need for increased gain and directivity, a requirement that cannot be achieved using a single element.

Nonetheless, the performance in terms of capacity remains consistent for both a single element and an array, as the array is processed through a singular port. The frequency channel is consistently occupied for a significant duration, yet the demand for high data rates remains unmet. The empirical evidence indicates that implementing 5G networks necessitates the utilization of broader bandwidth and Multiple-Input Multiple-Output (MIMO) technology. The recommendation made by the Federal Communications Commission (FCC) has initiated a subsequent research phase focused on the development of Multiple-Input Multiple-Output (MIMO) antennas tailored explicitly for the 5G cellular spectrum [6-9]. The frequency that is considered particularly favorable for 5G cellular communication is the 28 GHz band [10-14].

Additionally, an ongoing study for optimizing MIMO arrays specifically for this spectrum [15-19]. The dimensions of the antenna are contingent upon the specific operating frequency. The high-frequency antenna efficiently operates within a limited physical space and requires careful attention during development.

Microstrip patch array antennas are widely used as printed resonant antennas in narrowband microwave wireless communications. These antennas can be effectively simulated using various software tools such as CST and HFSS. The determining factors for the optimal solution mainly lie in the structure's geometric characteristics and the desired precision level. In the context of time-domain analysis, CST is considered the most optimal simulator for structures with simple geometries, such as circular or rectangular shapes. The Computational Electromagnetics (CEM) method known as CST employs the Finite Integration Technique (FIT), a reliable discretization scheme for Maxwell's equations in their integral formulation. The matrix equations that arise from the discretization of the fields can be employed to conduct numerical simulations with improved efficiency. Using a planar Microstrip patch antenna, which possesses a regular shape, suggests that CST is a suitable and more proficient simulator compared to alternative simulation tools.

2. MOTIVATION

The rapid progress in wireless communication system technology has resulted in a significant need to create novel antenna structures. The microstrip array antenna has a contemporary design within the wireless communication system, rendering it a captivating subject for research. This technology is prevalent within mobile communication, primarily aimed at augmenting the system's scope and dependability. The necessity to develop a beam antenna that is high-gain, compact, and directional arises from the heightened attenuation experienced by high frequencies.

In addition, a significant proportion of the microstrip antenna array exhibits considerable size. One of the primary constraints associated with the typical microstrip antenna array design pertains to maintaining a specific inter-element spacing to minimize mutual coupling effectively.

2.1 Illustrations of Performance parameter

A parametric investigation was undertaken to analyze the impact of various antenna parameters on impedance matching characteristics, hence facilitating an examination of the influence of these parameters on the impedance bandwidth. This work holds significance as it contributes to the comprehension of antenna features for individuals involved in antenna design. The study investigated the impact of altering the patch width (W) and the gap between the patch and the ground plane (hs) on impedance bandwidth. These parameters were the most influential factors in determining the system's susceptibility. Furthermore, an investigation was conducted to examine the impact of the inset feed gap, patch length, and width. In the simulations, all parameters except the parameter of interest were held constant.

The dimensions of the ground plane play a crucial role in the design of narrowband antennas with a finite ground plane, as they are highly sensitive characteristics. Numerous researchers have noticed a significant correlation between the impedance bandwidth and the presence of a ground plane.

2.1.1. Quality factor, Bandwidth, Gain, Efficiency

The antenna figure-of-merit encompasses the quality factor, bandwidth, and efficiency, all of which are interconnected. It is important to note that these parameters cannot be individually optimized as a whole. Hence, a trade-off between these factors is inevitable while striving for optimal antenna performance. Frequently, there exists an inclination to maximize one variable while concurrently diminishing the efficacy of the other.

The quality factor is a metric that quantifies the antenna losses, serving as a figure of merit. Commonly observed in various systems, there are several types of losses: radiation, conduction (also known as ohmic), dielectric, and surface wave losses. Hence, the cumulative impact of these losses significantly affects the overall quality factor Q_1 , which is commonly denoted as [21].

$$\frac{1}{Q_t} = \frac{1}{Q_{rad}} + \frac{1}{Q_c} + \frac{1}{Q_d} + \frac{1}{Q_{sw}} \quad \dots \quad \dots \quad 2.1$$

Where,

- Q_t = total quality factor
- Q_{rad} = quality factor due to radiation (space wave) losses
- Q_c = quality factor due to condition (ohmic) losses
- Q_d = quality factor due to dielectric losses
- Q_{sw} = quality factor due to surface waves

In the case of substrates with extremely low thickness, the losses attributed to surface waves are negligible and can be disregarded. Nevertheless, it is imperative to consider thicker substrates in the analysis. As mentioned earlier, the losses can be mitigated by utilizing cavities as described in references [14] and [15].

Approximate formulas represent the quality factors of different losses for thin substrates (where the thickness is much smaller than the wavelength) of arbitrary shapes, such as rectangular and circular shapes [21]. These concepts can be articulated as follows.

$$Q_c = h\sqrt{\pi f \mu \sigma} \quad \dots \quad \dots \quad \dots \quad 2.2$$

$$Q_d = \frac{1}{\tan \delta} \quad \dots \quad \dots \quad \dots \quad 2.3$$

$$Q_{rad} = \frac{2\omega\epsilon_r}{hG_t/l} K \quad \dots \quad \dots \quad \dots \quad 2.4$$

The symbol $\tan \delta$ represents the loss tangent of the substrate material, whereas σ denotes the conductivity of the conductors connected to the patch and ground plane. G_t/l represents the overall conductance per unit length of the radiating aperture.

The bandwidth of an antenna refers to the frequency range in which the antenna's performance, with respect to a specific attribute, meets a predetermined criterion. The bandwidth refers to the frequency range surrounding a central frequency within which the antenna's characteristics, including input impedance, pattern, beamwidth, polarization, sidelobe level, gain, beam direction, radiation, and efficiency, remain within an acceptable range. This acceptable range is determined by the ratio of the upper frequency to the lower frequency of operation.

As an illustration, a bandwidth ratio of 10:1 signifies that the top frequency is tenfold higher than the lower frequency. In the context of narrowband antennas, the bandwidth is commonly denoted as a proportion of the frequency deviation relative to the central frequency inside the bandwidth. For instance, a bandwidth of 5% signifies that the permissible range of frequencies for operation deviates by 5% from the center frequency of the bandwidth.

The fractional bandwidth of the antenna is inversely proportional to the Q_t of the antenna, and it is defined by

$$\frac{\Delta f}{f_0} = \frac{1}{Q_t} \quad \dots \quad \dots \quad 2.5$$

However, this approach may have limited utility as it fails to consider the important aspect of impedance matching at the input terminals of the antenna. A more comprehensive characterization of the fractional bandwidth pertains to a range of frequencies in which the Voltage Standing Wave Ratio (VSWR) at the input terminals is equal to or below the specified maximum threshold, assuming that the VSWR is unity at the designated frequency. A modified version of equation (2.5) that incorporates the consideration of impedance matching has been proposed in reference [21].

$$\frac{\Delta f}{f_0} = \frac{VSWR - 1}{Q_t \sqrt{VSWR}} \quad \dots \quad 2.6$$

In general, it is proportional to the volume, which for a rectangular microstrip antenna at a constant resonant frequency can be expressed as

$$BW \sim volume = area \cdot height = length \cdot width \cdot height$$

$$\sim \frac{1}{\sqrt{\epsilon_r}} \frac{1}{\sqrt{\epsilon_r}} \sqrt{\epsilon_r} = \frac{1}{\sqrt{\epsilon_r}} \quad \dots \quad \dots \quad 2.7$$

Hence, the relationship between the bandwidth and the dielectric constant of the substrate can be described as an inverse proportionality; namely, the bandwidth is inversely proportional to the square root of the dielectric constant. Figure 8 illustrates a standard representation of the bandwidth variation for a microstrip antenna with respect to the normalized height of the substrate. The relationship between substrate height and bandwidth is observed since an increase in substrate height leads to an increase in bandwidth.

The antenna's gain and directional capabilities: The gain of an antenna in a certain direction is defined as the ratio between the intensity of radiation in that direction and the intensity that would be observed if the power received by the antenna were radiated uniformly in all directions. The radiation intensity associated with the power radiated in all directions equally is equivalent to the power received by the antenna divided by 4π .

$$Gain = 4\pi \frac{\text{radiation intensity}}{\text{total input (accepted) power}} = 4\pi \frac{U(\theta, \phi)}{P_{in}} \text{ (dimensionless)} \quad \dots \quad 2.8$$

When the direction is not started, the power gain is usually taken in the direction of maximum radiation.

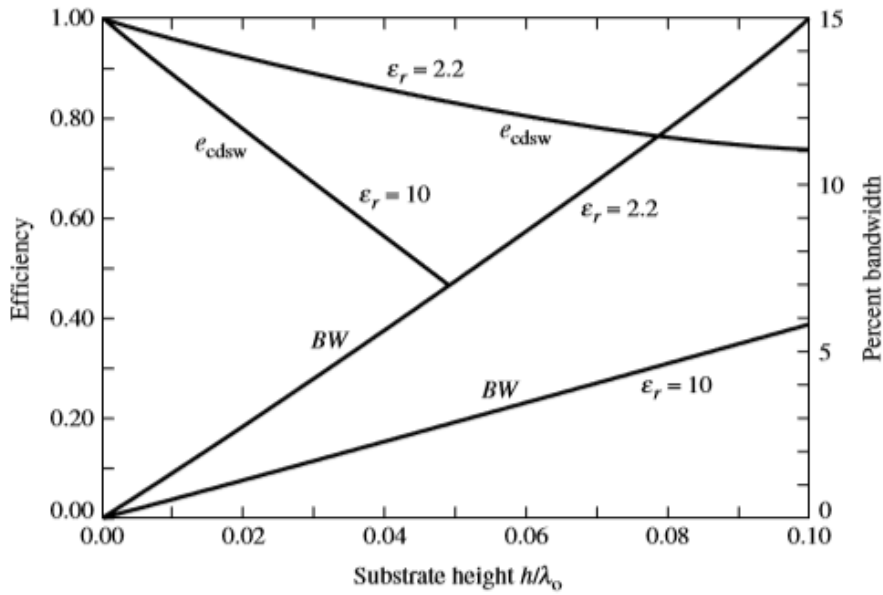


Figure 1: Efficiency and bandwidth versus substrate height at the resonant frequency for a rectangular microstrip patch for two different substrates. SOURCE: [23].

The efficiency of antenna radiation can be determined by evaluating the ratio between the radiated power and the input power absorbed by the antenna. Computing an antenna's conduction and dielectric losses poses significant challenges, often necessitating testing techniques. Separating these losses is a complex task, as they tend to be intertwined and are commonly combined to determine the overall efficiency of the antenna, known as the effective conductivity and dielectric (ECD) efficiency. The resistance R_L is employed to symbolize the losses associated with conduction and dielectric effects.

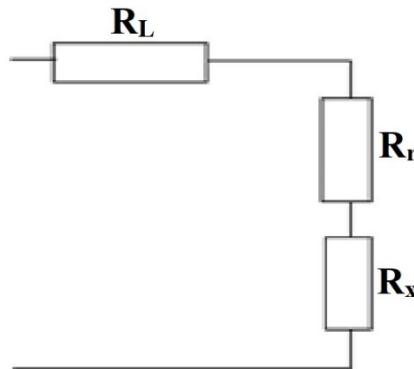


Figure 2: Conduction dielectric losses circuit.

The conduction-dielectric efficiency e_{cd} is defined as the ratio of the power delivered to the radiation resistance R_r to the power delivered to R_r and R_L , and the radiation efficiency can be written as

$$e_{cd} = \left[\frac{R_r}{R_L + R_r} \right] \quad (\text{dimensionless}) \quad \dots \quad 2.9$$

It is defined as the power radiated over the input power. It can also be expressed in terms of the quality factors, which for a microstrip antenna can be written as

$$e_{cdsw} = \left[\frac{1/Q_{rad}}{1/Q_t} = \frac{Q_t}{Q_{rad}} \right] \quad \dots \quad \dots \quad 2.10$$

Where Q_t is given by 2.1, typically, variations of the efficiency as a function of the substrate height for a microstrip antenna with two different substrates are shown in Figure 8.

2.1.2. MIMO Antenna Overview

The concept of multiple input refers to a scenario in which multiple sources of input or the several-output (MIMO) technique involves the simultaneous use of several antennas at both the transmitter and receiver. This technique allows for the independent transmission of signals from the transmit antennas.

The utilization of numerous antennas enhances the transmission capacity within the constraints of restricted bandwidth and power levels. According to reference [22], in an optimal scenario, the channel capacity is directly correlated with the quantity of transmitter and reception antennas in a multipath environment.

$$C = B \log_2(1 + M \times N \times SNR) \quad \dots \quad \dots \quad 2.11$$

where C is the channel capacity in bits/sec, B is the channel bandwidth in Hz, and M and N are the number of transmitter antennas and receiver antennas, respectively. SNR is the signal-to-noise ratio (absolute value). To be able to embed and integrate multiple antennas at the user terminal, size becomes a major limiting factor. The need for compact MIMO antennas with good performance metrics is thus a major task.

In addition to the standard metrics and characteristics used to assess antenna performance, such as bandwidth, resonance frequency, radiation patterns, gain, and efficiency, it is crucial to examine a few significant factors in order to define a Multiple-Input Multiple-Output (MIMO) antenna system. As mentioned earlier, the metrics are not seen as important in single-antenna devices. However, they are considered crucial in the case of multi-antenna systems.

3. METHODOLOGY

The rationale for developing a finite array antenna is to create a compact, straightforward antenna that exhibits minimal aberrations while offering adequate bandwidth. Initially, a resonance-focused patch was developed to operate at a frequency of 28 GHz. Subsequently, a two-element array was constructed utilizing the corporate feed technique, which evenly distributes the incoming power into two separate paths. Subsequently, enhancements were made to the system's architecture and performance, resulting in the construction of a six-element array. This array features the alignment of two corporate feeds in series with the basic corporate feed. The incident power is distributed into three pathways at each junction during each occurrence. After successfully achieving satisfactory simulated performance of the one-port array, a twelve-element two-port array was then designed utilizing the identical structure. The performance of this multiple-input multiple-output (MIMO) system was then tested by simulation using CST software.

The finite array antenna is fabricated on a single surface of a Rogers RT5880 printed circuit board (PCB) substrate, which has a thickness of 0.254 mm. The PCB substrate possesses a relative permittivity of 2.2 and a loss tangent of 0.0009. The patch and the ground thickness are measured to be 0.035 mm. The material used for both components is copper in an annealed state. The corporate feed designs in CST utilized the analytical line impedance calculation functionality to determine and modify the width of the microstrip feedline. This adjustment was made to provide adequate impedance matching for feedlines with resistances of 50, 70, and 100 ohms.

The geometric parameters necessary to reach a resonance frequency of 28 GHz were computed and utilized in the design of a single patch. Subsequently, the patch's dimensions were further refined to attain the requisite resonance and performance characteristics. The configuration of the single patch is seen in Figure 13. The optimized parameters of the single patch are listed in Table 2.1. The geometric parameters of the single patch structure can be adjusted to achieve the desired resonance.

Table-2.1 Dimension list of the Single patch antenna:

Dimension	Name	Value
Patch Width	W	3.46 mm
Patch Length	L	4.25 mm
Length of the Substrate	Lg	4.984 mm
Width of the Substrate	Wg	5.774 mm
Height of the substrate	hs	0.254 mm
Thickness of radiator	ht	0.035 mm
Length of feedline	Lf	1.73 mm
Length of inset	Fi	0.968 mm
The gap between the inset	Gpf	0.25 mm

Figure 3 illustrates the single patch antenna's 3D view and surface current.

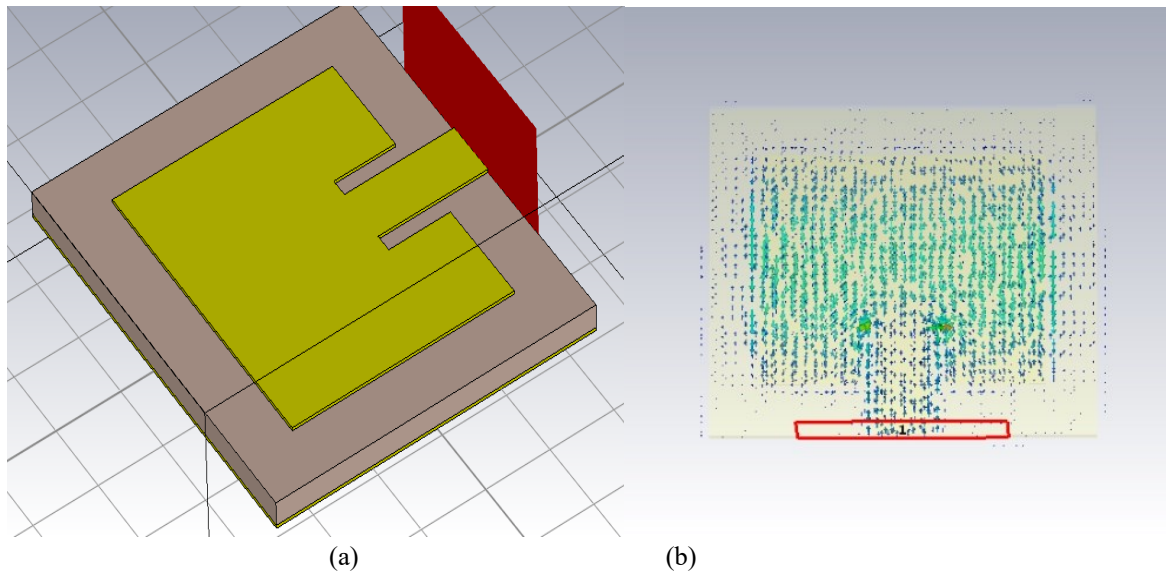


Figure 3: (a) 3D view and (b) Surface Current of the single patch antenna

The current distribution figure shows that the maximum area of the designed antenna is packed with current intensity and current density is at maximum right in the middle of the patch antenna, which is essential for efficient radiation.

The 6-element array is arranged side by side to establish a 12-element array powered by two waveguide ports to evaluate the array's MIMO performance. The spacing between a couple of arrays is 1.524 mm wide. In Figure 13, the 3D structure of the 12-element array is demonstrated.

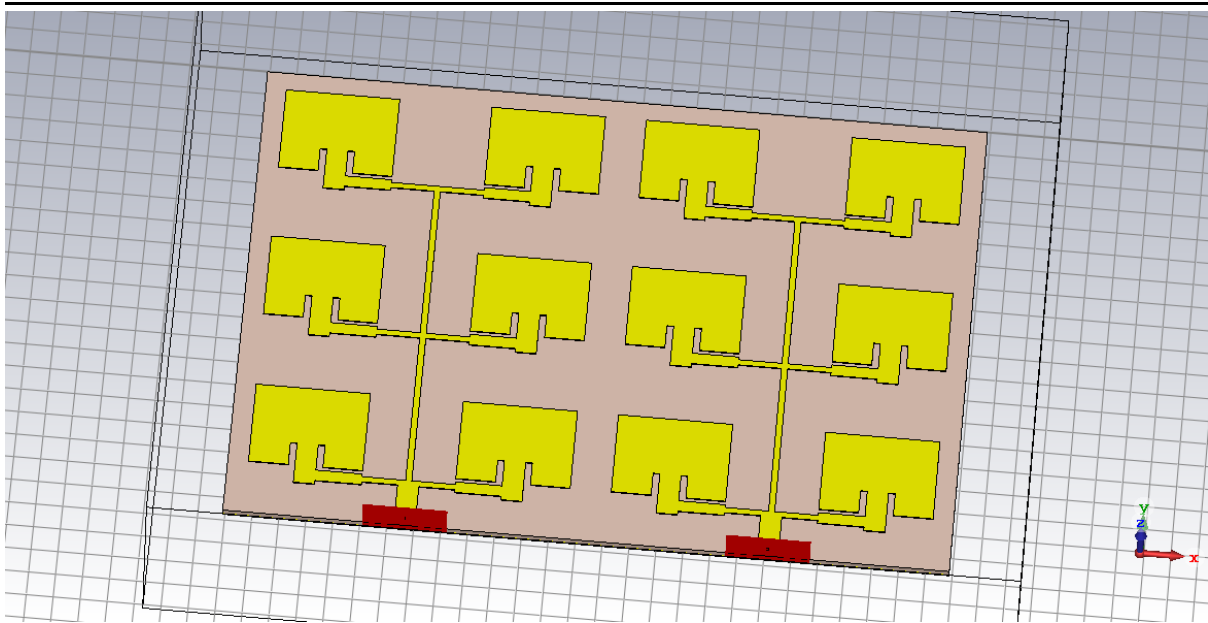


Figure 4: 3D structure of the 12-element 2-port array.

The overall dimensions for the substrate and ground of the one-port array and two-port array are categorized and listed in Table 2.2.

Table-2.2 Overall ground and substrate dimensions of the single array and the MIMO array:

Component	6 element array		12 element MIMO array	
	Length	Width	Length	Width
Substrate	19.99 mm	13.484 mm	19.99 mm	26.968 mm
Ground	19.99 mm	13.484 mm	19.99 mm	26.968 mm

The surface current of the 12-element array is portrayed in Figure 13.

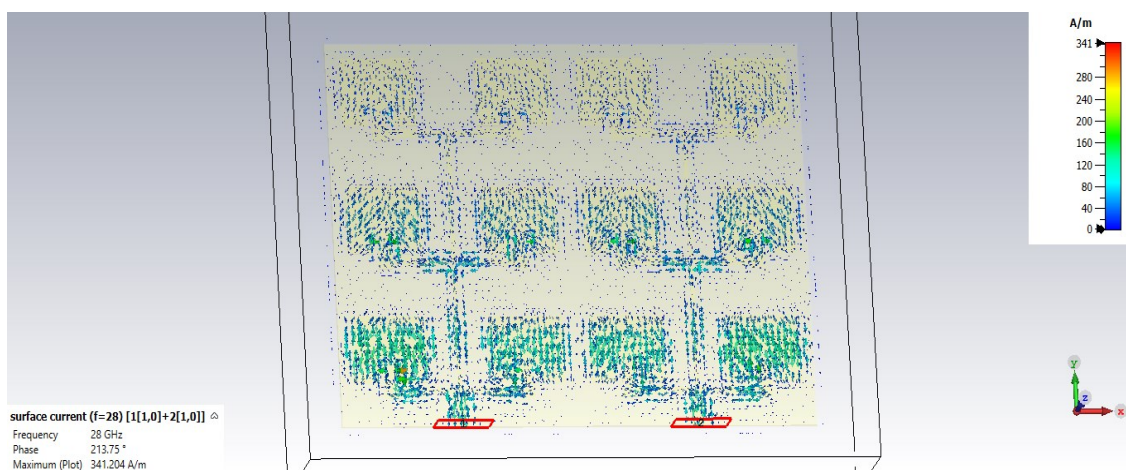


Figure 5: Current distribution on the surface of the array antenna

As the figure shows, The current density and intensity of the array are relatively similar to the single port six-element array.

4. RESULT AND DISCUSSION

The performance of the proposed antenna array was evaluated and enhanced using the Finite Integration Technique within the CST microwave simulator. The parameters utilized in the analysis included dimensions obtained from equations and approximations (in the case of corporate feed). Subsequently, the parameters were optimized to improve the simulation results for return loss, VSWR, impedance characteristics, radiation pattern, and other relevant factors. This study evaluates simulated bandwidth, gain, efficiency, and MIMO performance of the corporate-fed two-port, 12-element array antenna. The assessment is conducted subsequent to the construction and design of the antenna.

VSWR parameter defines how well the antenna impedance matches the transmission line by taking the ratio of the reflected maximum and minimum voltage wave. A value of $VSWR \leq 2$ is considered the primary requirement.

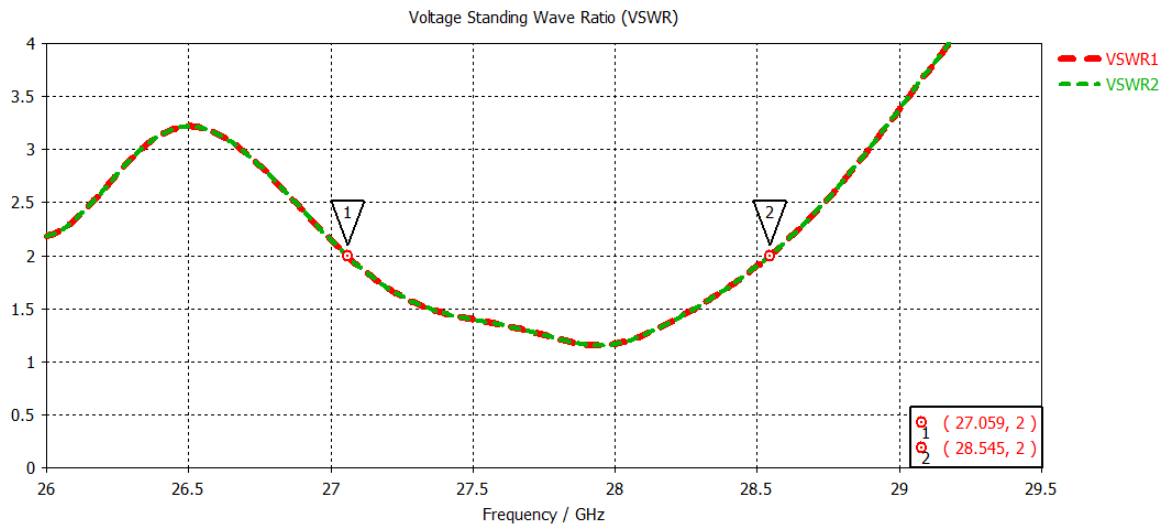


Figure 6: VSWR of the proposed array antenna

The plots of the VSWR of the proposed antenna in Fig. 16 show that the measured impedance bandwidth of the proposed antenna is 28 GHz for $VSWR \leq 2$. Figure 7 demonstrates that the proposed antenna's reflection coefficients S_{11} and S_{22} are below -10dB, resonating in the mmWave frequency spectrum ranging from 27.09 to 28.51 GHz with a 1.42 GHz bandwidth.

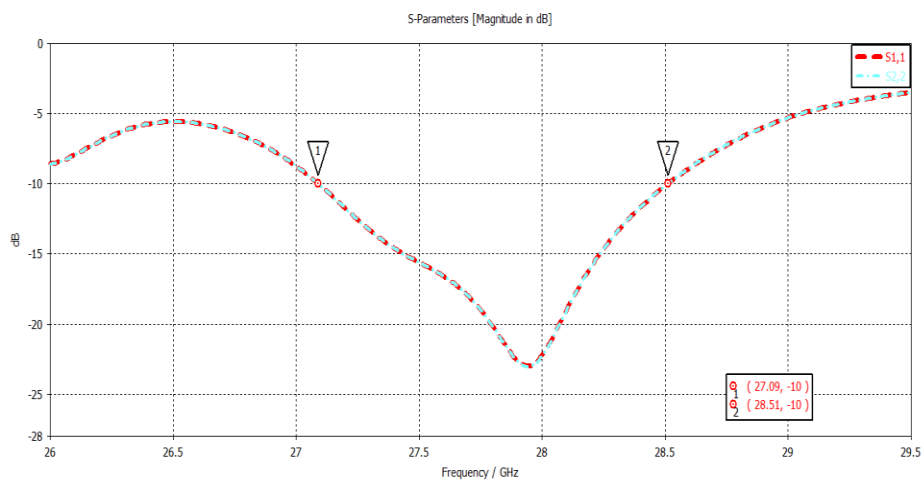


Figure 7: Reflection coefficient of the proposed array antenna

Figure 8 illustrates the transmission coefficients of the proposed antenna, which shows satisfactory isolation between the antenna ports. Where, $S_{12} = S_{21} < -20$ dB

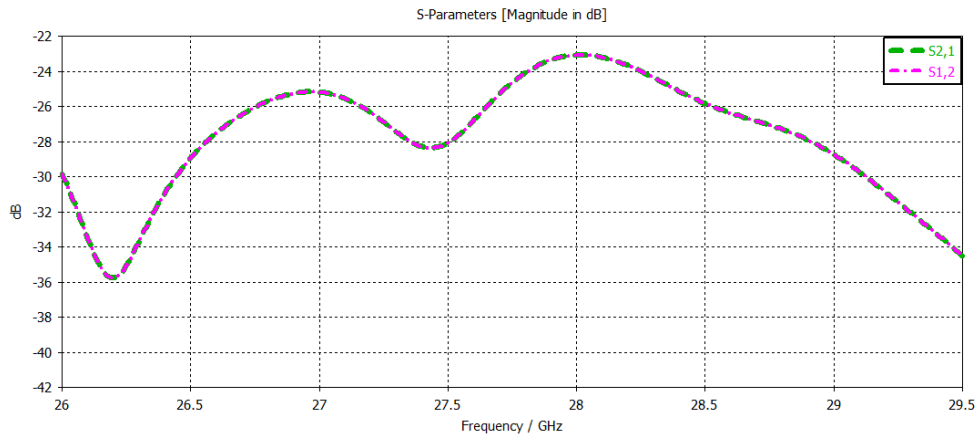


Figure 8: Transmission coefficient of the proposed array antenna

Radiation is the term used to represent the emission or reception of wave-front at the antenna, specifying its strength. Radiation Patterns are diagrammatical representations of the distribution of radiated energy into space as a function of direction.

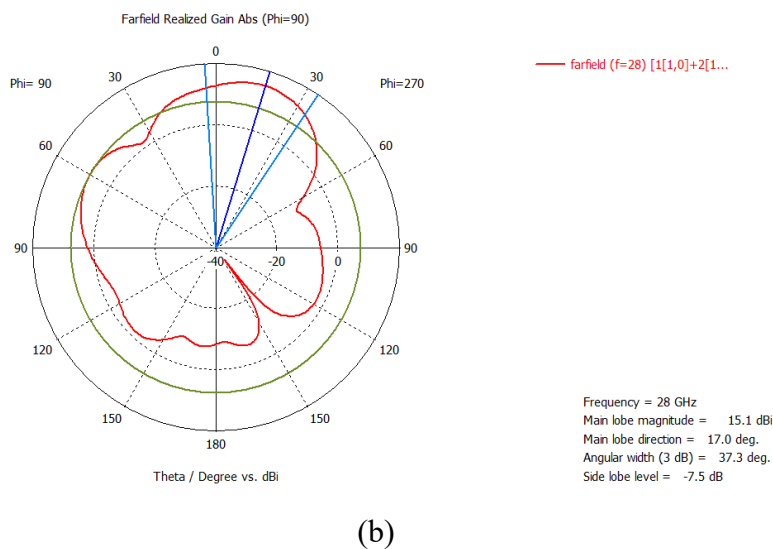
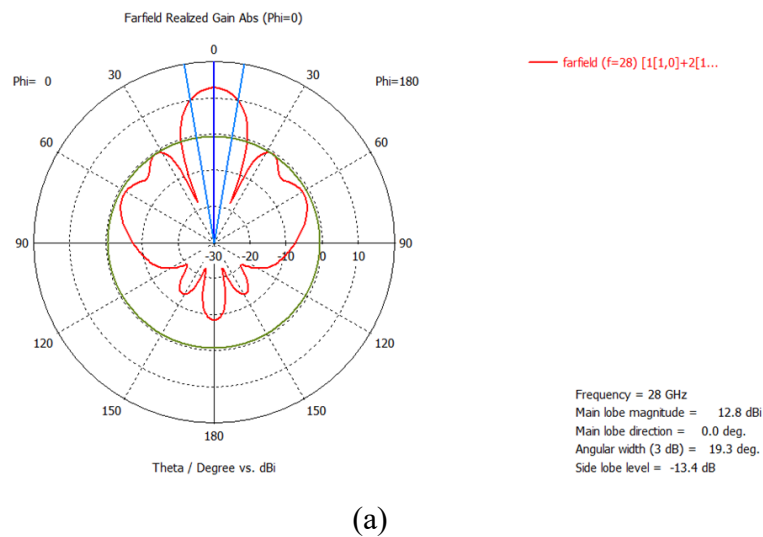


Figure 9: 1D Far-field radiation pattern at 28GHz for (a) $\Phi=0^\circ$, (b) $\Phi=90^\circ$.

Figure 9 shows the 1D radiation pattern at 28 GHz with a main lobe magnitude of 12.8 dBi in realized gain with angular width of 19.3° for $\Phi=0^\circ$ (XZ plane) and main lobe magnitude of 15.1 dBi in realized gain with main lobe direction of 17° for $\Phi=90^\circ$ (YZ plane). Figure 21 shows the 3D radiation pattern of the proposed antenna in the XZ and YZ planes, illustrating that it is a directional antenna.

A comparison of the proposed antenna design with related works reported in the literature is listed in Table 4.1. The comparative analysis with other works shows that the proposed design demonstrates moderate compactness, bandwidth and gain performance. MIMO performance analysis is provided in detail for the proposed design, and it is observed that the MIMO antenna proposed in this work exhibits better performance as compared to other reported results. The suitability of the proposed MIMO array antenna for 28GHz mm-wave applications are established.

Table - 4.1 Performance comparison of this proposed antenna design with other recent works.

Reference	Frequency (GHz)	Board Size (mm ³)	No. of Ports	Bandwidth (GHz)	Gain (dBi)	ECC	Diversity Gain(dB)
[31]	3.6	150 × 75 × 1.6	8	1.2	2.5	<0.01	—
[32]	28	41.3 × 46 × 0.5	4	3.35	13.1	—	—
[33]	24	15 × 19 × 0.254	2	0.8	6	0.24	9.7
[34]	5.2 & 24	40 × 25 × 0.254	2	0.1 & 0.77	5 & 7.3	—	—
[35]	28	20 × 20 × 0.254	2	0.85	8	0.13	9.9
This work	28	19.99 × 26.96 × 0.254	2	1.42	12.2	<0.01	10

5. CONCLUSION

The utilization of mmWave frequency bands is anticipated to address the current limited spectrum in wireless cellular networks. This study analyzes a planar patch antenna with a bandwidth of 1.42 GHz, which covers the 28 GHz 5G spectrum. The analysis includes a two-port 12-element MIMO configuration implemented on a Rogers RT Duroid 5880 substrate measuring $19.99 \times 26.96 \times 0.254$ mm³. The MIMO array antenna demonstrates a simple and compact structure, enabling operation within the frequency range of 27.09 GHz to 28.52 GHz. The measured peak gain for the proposed design is 12.3 dBi. Simulation results indicate a moderate impedance bandwidth with excellent matching and high isolation. Furthermore, the MIMO performance criteria, including a low ECC value, are satisfied. Consequently, the proposed architecture is suitable for future high-data-rate wireless networks.

REFERENCES

- [1] Pramod Dhande, "Antennas and its Applications", Armament Research & Development Establishment, Dr. Homi Bhabha Rd, Pashan, Pune.
- [2] W. F. Williams, "High-Efficiency Antenna Reflector", Microwave Journal, Vol. 8, July 1965.
- [3] David Alvarez Outerelo, Ana Vazquez Alejos, Manuel Garcia Sanchez, Maria Vera Isasa, "Microstrip Antenna for 5G Broadband Communications: Overview of Design Issues", Department of Teoria de la Señal y Comunicaciones University of Vigo Vigo, Pontevedra, Spain.
- [4] Y. Niu, Y. Li, D. Jin, L. Su, and A. V. Vasilakos, "A survey of millimeter wave communications (mmwave) for 5g: opportunities and challenges," Wireless Networks, vol. 21, no. 8, pp. 2657–2676, 2015.
- [5] S. F. Jilani and A. Alomainy, "A Multiband Millimeter-Wave TwoDimensional Array Based on Enhanced Franklin Antenna for 5G Wireless Systems," IEEE Antennas and Wireless Propagation Letters, 2017.

-
- [6] X. Zhao, S. P. Yeo, and L. C. Ong, "Planar UWB MIMO Antenna With Pattern Diversity and Isolation Improvement for Mobile Platform Based on the Theory of Characteristic Modes," *IEEE Transactions on Antennas and Propagation*, vol. 66, no. 1, pp. 420–425, 2018.
- [7] N. Ashraf, O. M. Haraz, M. M. M. Ali, M. A. Ashraf, and S. A. S. Alshebili, "Optimized broadband and dual-band printed slot antennas for future millimeter wave mobile communication," *AEU-International Journal of Electronics and Communications*, vol. 70, no. 3, pp. 257–264, 2016.
- [8] Y. A. Hashem, O. M. Haraz, and E.-D. M. El-Sayed, "6-Element 28/38 GHz dual-band MIMO PIFA for future 5G cellular systems," in *Antennas and Propagation (APSURSI), 2016 IEEE International Symposium on. IEEE, 2016*, pp. 393–394
- [9] M. Ikram, M. Sharawi, K. Klionovski, and A. Shamim, "A switchedbeam millimeter-wave array with MIMO configuration for 5G applications," *Microwave and Optical Technology Letters*, vol. 60, no. 4, pp. 915–920, 2018.
- [10] D.M. Pozar, "Microstrip Antennas," *Proc. IEEE*, Vol. 80, No. 1, January 1992. © 1992 IEEE.
- [11] W. F. Richards, Y. T. Lo, and D. D. Harrison, "An Improved Theory of Microstrip Antennas with Applications", *IEEE Trans. Antenna Propagat.*, Vol. AP-29, No. 1, January 1981.
- [12] C. M. Krowne, "Cylindrical-Rectangular Microstrip Antenna", *IEEE Trans. Antenna Propagat.*, Vol. AP-31, No. 1, January 1983.
- [13] S. B. De Assis Fonseca and A. J. Giarola, "Microstrip Disk Antennas, Part 1: Efficiency of Space Wave Launching", *IEEE Trans. Antenna Propagat.*, Vol. AP-29, No. 1, June 1984.
- [14] R. J. Mailloux, "On the Use of Metallized Cavities in Printed slot Arrays with Dielectric Substrates", *IEEE Trans. Antenna Propagat.*, Vol. AP-35, May 1987.
- [15] J. T. Aberle and F. Zavosh, "Analysis of Probe-Fed Circular Microstrip Patches Backed by Circular Cavities", *IEEE Trans. Electromagnetics*, Vol. AP-14, 1994.
- [16] A. Henderson, J. R. James, and C. M. Hall, "Bandwidth Extension Techniques in Printed Conformal Antennas", *Military Microwaves*, Vol. MM 86, 198
- [17] D. M. Pozar and B. Kaufman, "Increasing the Bandwidth of a Microstrip Antenna by Proximity Coupling", *Electrical Letters*, Vol. 23, April 1987.
- [18] D. M. Pozar and D.H. Schaubert, "Scan Blindness in Infinite Phased Arrays of printed Dipoles", *IEEE Trans. Antennas Propagat.*, Vol. AP-32, June 1984.
- [19] Indrasen Singh, Dr. V. S. Tripathi, "Microstrip Patch Antenna and its Application", *Int. J. Comp. Tech. Appl.*, Vol 2(5), September 2011.
- [20] Ramesh Garg, Prakash Bartia, Inder Bahl, Apisak Ittipiboon, "Microstrip Antenna Design Handbook", Artech House Inc. Norwood, MA, 2001.
- [21] K. R. Carver and J. W. Mink, "Microstrip Antenna Technology", *IEEE Trans. Antennas Propagat.*, Vol. AP-29, January 1981.
- [22] Y T Lo and S W Lee, "Antenna Handbook Theory, Applications & Design", Van Nostrand Rein Company, NY, 1997.
- [23] A. G. Derneryd, "Linearly Polarized Microstrip Antennas", *IEEE Trans. Antennas Propagat.*, Vol. AP-24, November 1976.
-